Cell Reports

Article

SPT16 ubiquitylation by DCAF14-CRL4 regulates FACT binding to histones

Graphical abstract

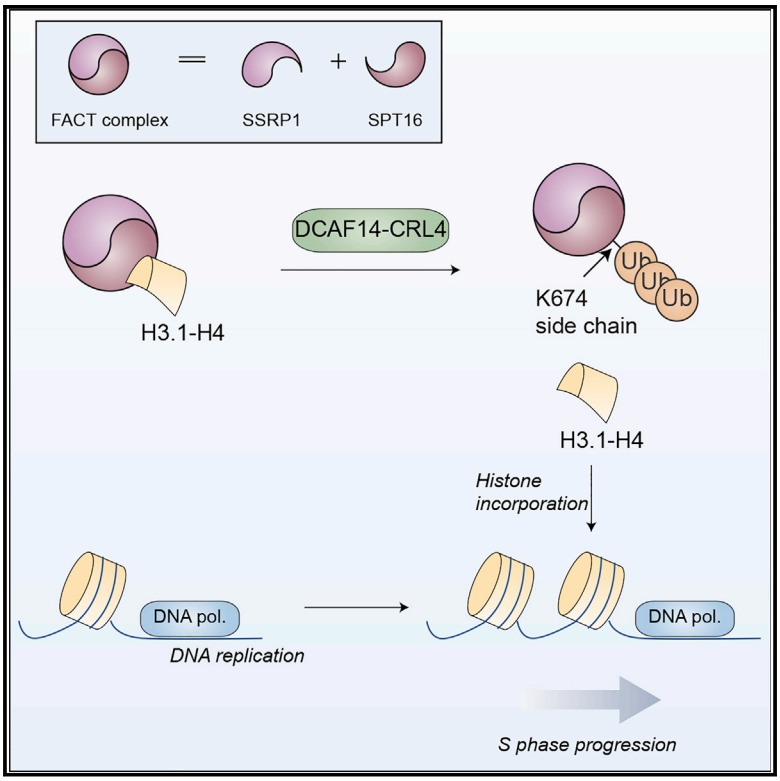

Highlights

- The SPT16 subunit of the FACT complex is ubiquitylated at K674
- The ubiquitin ligase DCAF14-CRL4 is responsible for SPT16 ubiquitylation
- Ubiquitylation of SPT16 inhibits its binding to histone H3.1
- SPT16 ubiquitylation increases the level of H3.1 in chromatin during S phase

Authors

Tadashi Nakagawa, Akane Morohoshi, Yuko Nagasawa, ..., Yasuhiro Noda, Toru Hosoi, Keiko Nakayama

Correspondence

nakayak2@med.tohoku.ac.jp

In brief

The histone chaperone FACT plays a role in DNA replication, transcription, and repair, but its regulation is unclear. Nakagawa et al. report that DCAF14-CRL4 ubiquitylates the FACT subunit SPT16 and that such ubiquitylation may regulate DNA replication-coupled histone incorporation into chromatin and thereby ensure efficient S-phase progression.

Nakagawa et al., 2022, Cell Reports *38*, 110541
March 22, 2022
https://doi.org/10.1016/j.celrep.2022.110541

CellPress

Cell Reports

CellPress
OPEN ACCESS

Article

SPT16 ubiquitylation by DCAF14-CRL4 regulates FACT binding to histones

Tadashi Nakagawa,[1,2,3] Akane Morohoshi,[1,3] Yuko Nagasawa,[1] Makiko Nakagawa,[1] Masaki Hosogane,[1] Yasuhiro Noda,[2] Toru Hosoi,[2] and Keiko Nakayama[1,4,*]

[1]Division of Cell Proliferation, ART, Graduate School of Medicine, Tohoku University, Sendai, Miyagi 980-8575, Japan

[2]Department of Clinical Pharmacology, Faculty of Pharmaceutical Sciences, Sanyo-Onoda City University, Sanyo-Onoda, Yamaguchi 756-0884, Japan

[3]These authors contributed equally

[4]Lead contact

*Correspondence: nakayak2@med.tohoku.ac.jp

https://doi.org/10.1016/j.celrep.2022.110541

SUMMARY

The histone chaperone complex FACT comprises SPT16 and SSRP1 and contributes to DNA replication, transcription, and repair, but how it plays such various roles is unclear. Here, we show that human SPT16 is ubiquitylated at lysine-674 (K674) by the DCAF14-CRL4 ubiquitin ligase. K674 is located in the middle domain of SPT16, and the corresponding residue of the yeast ortholog is critical for binding to histone H3.1-H4. We show that the middle domain of human SPT16 binds to histone H3.1-H4 and that this binding is inhibited by K674 ubiquitylation. Cells with heterozygous knockin of a K674R mutant of SPT16 manifest reduction of both SPT16 ubiquitylation and H3.1 in chromatin, a reduced population in mid S phase, impaired proliferation, and increased susceptibility to S phase stress. Our data thus indicate that SPT16 ubiquitylation by DCAF14-CRL4 regulates FACT binding to histones and may thereby control DNA replication-coupled histone incorporation into chromatin.

INTRODUCTION

Eukaryotic DNA is packaged into chromatin, the basic unit of which is the nucleosome, a structure comprising two sets of four core histone molecules (H2A, H2B, H3, and H4) surrounded by 146 bp of double-stranded DNA (Luger et al., 1997). The repair, replication, and transcription of genomic DNA require the recruitment of a variety of proteins. Although the access of these proteins to DNA is impeded by chromatin structure, dynamic changes in this structure allow these DNA-based processes to occur. Regulators of chromatin structure include histone-modifying (Bannister and Kouzarides, 2011) and DNA-modifying (Greenberg and Bourc'his, 2019; Wu and Zhang, 2017) enzymes, histone variants (Martire and Banaszynski, 2020), ATP-dependent chromatin-remodeling complexes (Clapier et al., 2017), and histone chaperones (Gurard-Levin et al., 2014; Hammond et al., 2017).

Histone chaperones directly bind to histones and regulate their incorporation into and removal from chromatin in a manner independent of ATPase activity. The histone chaperone complex FACT (facilitates chromatin transcription/transaction) is a heterodimer composed of SPT16 and SSRP1 proteins in mammalian cells (and a heterotrimer of Spt16, Pob3, and Nhp6 in budding yeast) and is essential for cell survival (Gurova et al., 2018; Winkler and Luger, 2011). It was identified as indispensable for overcoming the block to RNA polymerase II-mediated transcript elongation imposed by chromatin DNA, whereas it is not required for transcription of naked DNA (Orphanides et al., 1998), and subsequent studies revealed that it plays an essential role not only in transcription but also in DNA replication and repair. However, the molecular mechanisms underlying the coordination of these activities of FACT have remained unclear.

Ubiquitylation is a reversible posttranslational protein modification characterized by covalent attachment of the 76-amino acid protein ubiquitin to a substrate protein (Nakagawa and Nakayama, 2015; Nakayama and Nakayama, 2006). Protein ubiquitylation consists of three steps catalyzed by an E1 ubiquitin-activating enzyme, an E2 ubiquitin-conjugating enzyme, and an E3 ubiquitin ligase, the last of which is responsible for substrate selection (Glickman and Ciechanover, 2002; Hershko and Ciechanover, 1998). Mammalian cells are estimated to contain 500 to 1,000 ubiquitin ligases, which are largely classified as either HECT-type or RING-type enzymes on the basis of the structure of the domain responsible for the ubiquitylation reaction (Deshaies and Joazeiro, 2009; Metzger et al., 2012; Rotin and Kumar, 2009). Ubiquitin ligases of the Cullin family (Cullin-RING ubiquitin ligases, or CRLs) constitute the largest group of RING-type enzymes, which outnumber HECT-type ubiquitin ligases. However, Cullin-family proteins (CUL1, -2, -3, -4A, -4B, 5, −7, and −9 in mammalian cells) do not possess ubiquitin ligase activity by themselves; instead, they associate with a RING domain protein (ROC1 or ROC2), an adaptor protein (DDB1 in the case of CUL4), and a substrate recognition protein (DCAF [DDB1 and CUL4-associated factor] proteins in the case

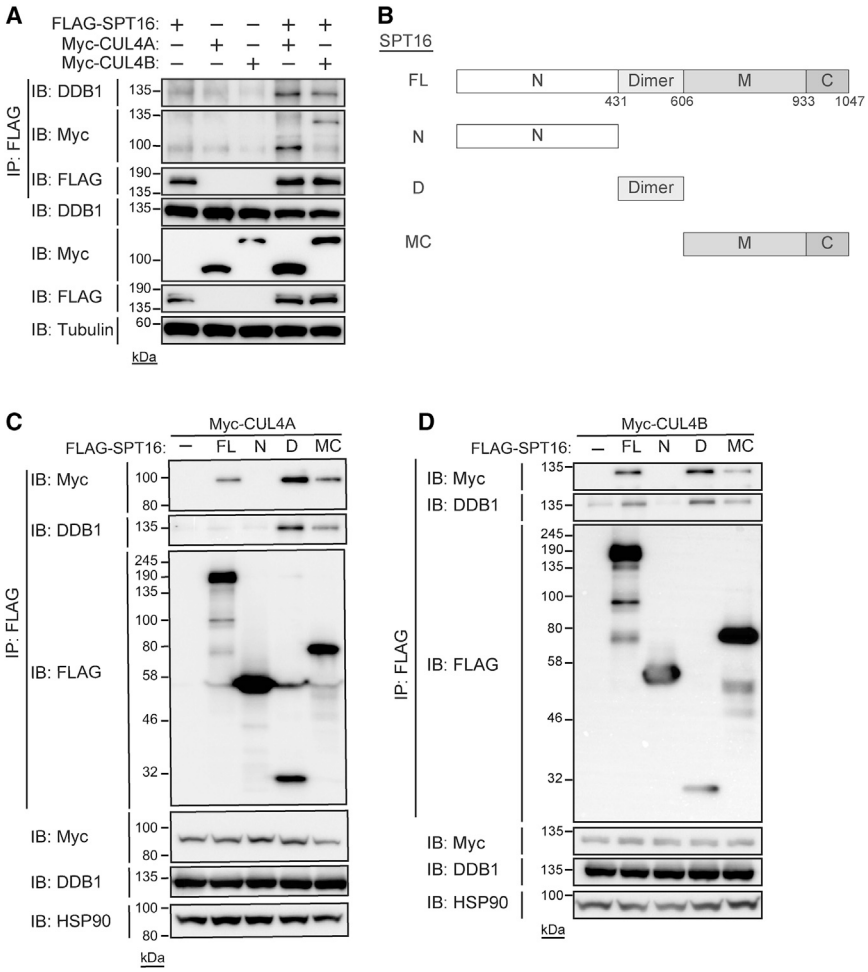

Figure 1. The CRL4 ubiquitin ligase binds to SPT16

(A) Lysates of HeLa cells transfected with the indicated combinations of expression plasmids for FLAG-SPT16 and either Myc-CUL4A or Myc-CUL4B were subjected to immunoprecipitation (IP) with antibodies to FLAG, and the resulting precipitates as well as the original cell lysates were subjected to immunoblot analysis (IB) with the indicated antibodies (tubulin was examined as a loading control). The images are representative of two independent experiments.

(B) Domain structure of full-length (FL) human SPT16 as well as the structure of NH_2-terminal domain (N, amino acids 1–431), dimerization domain (D, amino acids 432–606), and middle and COOH-terminal domain (MC, amino acids 607–1047) truncation mutants.

(C and D) Lysates of HeLa cells transfected with expression plasmids for FLAG-tagged FL or mutant forms of SPT16 as well as for either Myc-CUL4A (C) or Myc-CUL4B (D) were subjected to immunoprecipitation with antibodies to FLAG, and the resulting precipitates as well as the original cell lysates were subjected to immunoblot analysis with the indicated antibodies (HSP90 was examined as a loading control). The images are representative of two independent experiments. See also Figure S1.

of CUL4) in order to form an active ubiquitin ligase complex (Jackson and Xiong, 2009; Petroski and Deshaies, 2005). Among the eight mammalian Cullins, CUL1, CUL3, and CUL4 (Rtt101 in budding yeast) are conserved in yeast (Sarikas et al., 2011).

Ubiquitylation of Spt16 by the Rtt101 ubiquitin ligase complex was shown to result in the recruitment of FACT to replication origins and to facilitate DNA replication in budding yeast (Han et al., 2010). However, how origin-localized FACT facilitates DNA replication and whether this mechanism is conserved in mammalian cells have remained unclear. We here investigated the potential ubiquitylation of SPT16 and its relevance to cell proliferation in mammalian cells. Our results suggest that ubiquitylation of SPT16 by the DCAF14-CRL4 ubiquitin ligase complex is critical for the regulation of histone incorporation into chromatin during S phase of the cell cycle.

RESULTS

The CRL4 ubiquitin ligase associates with SPT16

Given that the Rtt101 ubiquitin ligase complex interacts with and ubiquitylates Spt16 in budding yeast (Han et al., 2010), we examined the possible role of CUL4, the mammalian ortholog of Rtt101, in SPT16 ubiquitylation. Mammalian cells express two isoforms of CUL4, with CUL4A and CUL4B sharing 80% amino acid sequence identity (Hannah and Zhou, 2015; Jackson and Xiong, 2009). Both CUL4A and CUL4B associate with the adaptor protein DDB1 to recruit substrates and substrate recognition proteins. To test whether SPT16 binds to DDB1 and CUL4, we transfected HeLa cells with expression plasmids for FLAG epitope-tagged human SPT16 and Myc epitope-tagged forms of human CUL4A or CUL4B. Immunoprecipitation of cell extracts with antibodies to FLAG followed by immunoblot analysis revealed that SPT16 interacted with Myc-CUL4A, Myc-CUL4B, and endogenous DDB1 (Figures 1A and S1A). Similar experiments with a series of deletion mutants of SPT16 showed that the dimerization domain (which binds to SSRP1) and the COOH-terminal portion of SPT16 are responsible for binding to CUL4A and CUL4B as well as to DDB1 (Figures 1B–1D).

The CRL4 ubiquitin ligase mediates SPT16 ubiquitylation

Whereas Spt16 was shown to be ubiquitylated in budding yeast, Pob3 was not (Han et al., 2010). To determine whether the mammalian FACT components SPT16 and SSRP1 are ubiquitylated, we transiently transfected HEK293T cells with expression vectors for hemagglutinin epitope (HA)-tagged ubiquitin and either FLAG-SPT16 or FLAG-SSRP1 and subjected cell extracts to immunoprecipitation with antibodies to FLAG under denaturing conditions. Immunoblot analysis of

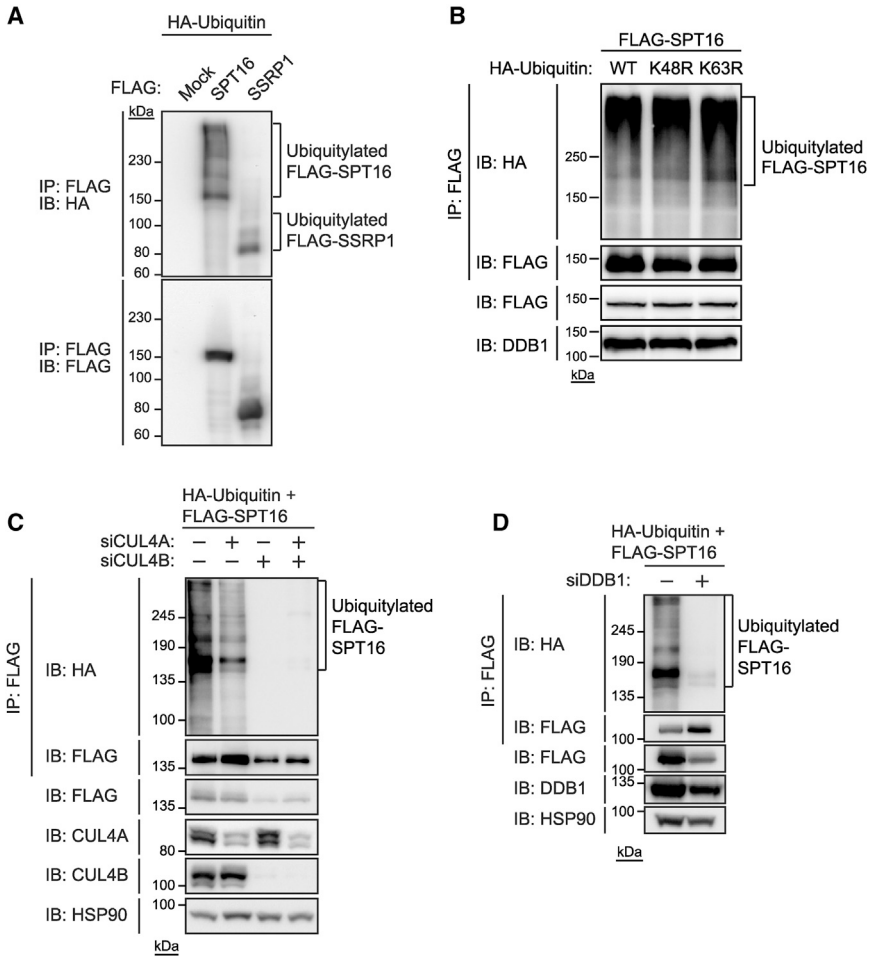

Figure 2. SPT16 is a substrate of a CRL4 ubiquitin ligase

(A) HEK293T cells transfected with expression plasmids for HA-ubiquitin and either FLAG-SPT16 or FLAG-SSRP1 were subjected to IP with antibodies to FLAG under denaturing conditions, and the resulting precipitates were subjected to IB analysis with antibodies to HA and to FLAG. The images are representative of two independent experiments.

(B) HEK293T cells transfected with expression plasmids for FLAG-SPT16 and HA-tagged WT or K48R or K63R mutant forms of ubiquitin were subjected to IP with antibodies to FLAG under denaturing conditions, and the resulting precipitates as well as the original cell lysates were subjected to IB analysis with the indicated antibodies. The images are representative of two independent experiments.

(C) HeLa cells transfected with CUL4A or CUL4B siRNAs as well as with expression plasmids for FLAG-SPT16 and HA-ubiquitin were subjected to IP with antibodies to FLAG under denaturing conditions. The resulting precipitates as well as the original cell lysates were then subjected to IB analysis with the indicated antibodies. The images are representative of two independent experiments.

(D) HeLa cells transfected with DDB1 siRNA and expression plasmids for FLAG-SPT16 and HA-ubiquitin were subjected to IP with antibodies to FLAG under denaturing conditions, and the resulting precipitates as well as the original cell lysates were subjected to IB analysis with the indicated antibodies. The images are representative of two independent experiments.

See also Figures S1 and S2.

the precipitated proteins with antibodies to HA revealed smeared ubiquitylation signals for SPT16, indicating that SPT16 is polyubiquitylated (Figures 2A and S1B). In addition, we detected distinct bands for both SPT16 and SSRP1 at positions corresponding to a molecular size ~10 to 20 kDa greater than that of the unmodified proteins, suggesting that SPT16 and SSRP1 are mono- or diubiquitylated (Figure 2A). Proteomics analysis has revealed the coexistence of all possible ubiquitin-ubiquitin linkages (K6, K11, K27, K29, K33, K48, K63, and the NH_2-terminal methionine residue M1) in mammalian cells (Akutsu et al., 2016; Swatek and Komander, 2016). The most prevalent and best-characterized such linkage is K48, with K48-linked ubiquitin chains serving to target proteins to the proteasome for degradation, whereas the second most abundant type of linkage, that mediated by K63, plays a role in nondegradative signal transduction. To explore which type of ubiquitin chain is attached to SPT16, we expressed HA-tagged ubiquitin mutants in which K48 or K63 had been changed to arginine (K48R or K63R, respectively), together with FLAG-SPT16, in HEK293T cells. The extent of SPT16 ubiquitylation did not differ between cells expressing either K48R or K63R mutant forms of ubiquitin and those expressing wild-type (WT) ubiquitin (Figure 2B), suggesting that the ubiquitin chain attached to SPT16 is not exclusively linked via K48 or K63. To scrutinize further the topology of the ubiquitin chain on SPT16, we examined the ubiquitylation of SPT16 in HEK293T cells expressing ubiquitin with each of the possible intramolecular ubiquitylation sites individually mutated (K6R, K11R, K27R, K29R, K33R, K48R, or K63R). We did not detect a substantial decrease in the ubiquitylation level of SPT16 with any of these ubiquitin mutants (Figure S2), indicating that the ubiquitin chain on SPT16 is branched.

To determine whether a CRL4 ubiquitin ligase complex is responsible for SPT16 ubiquitylation, we transfected HeLa cells first with small interfering RNAs (siRNAs) that target CUL4A or CUL4B mRNAs and then with expression vectors for FLAG-SPT16 and HA-ubiquitin. Knockdown of either CUL4A or CUL4B resulted in a substantial reduction in the ubiquitylation level of SPT16 (Figure 2C), suggesting that both CUL4A and CUL4B are required for ubiquitylation of the overexpressed SPT16. A reduction in the extent of SPT16 ubiquitylation was also observed in cells transfected with a siRNA that targets DDB1 mRNA (Figure 2D). These results thus suggested that SPT16 is a substrate of a CRL4 ubiquitin ligase complex.

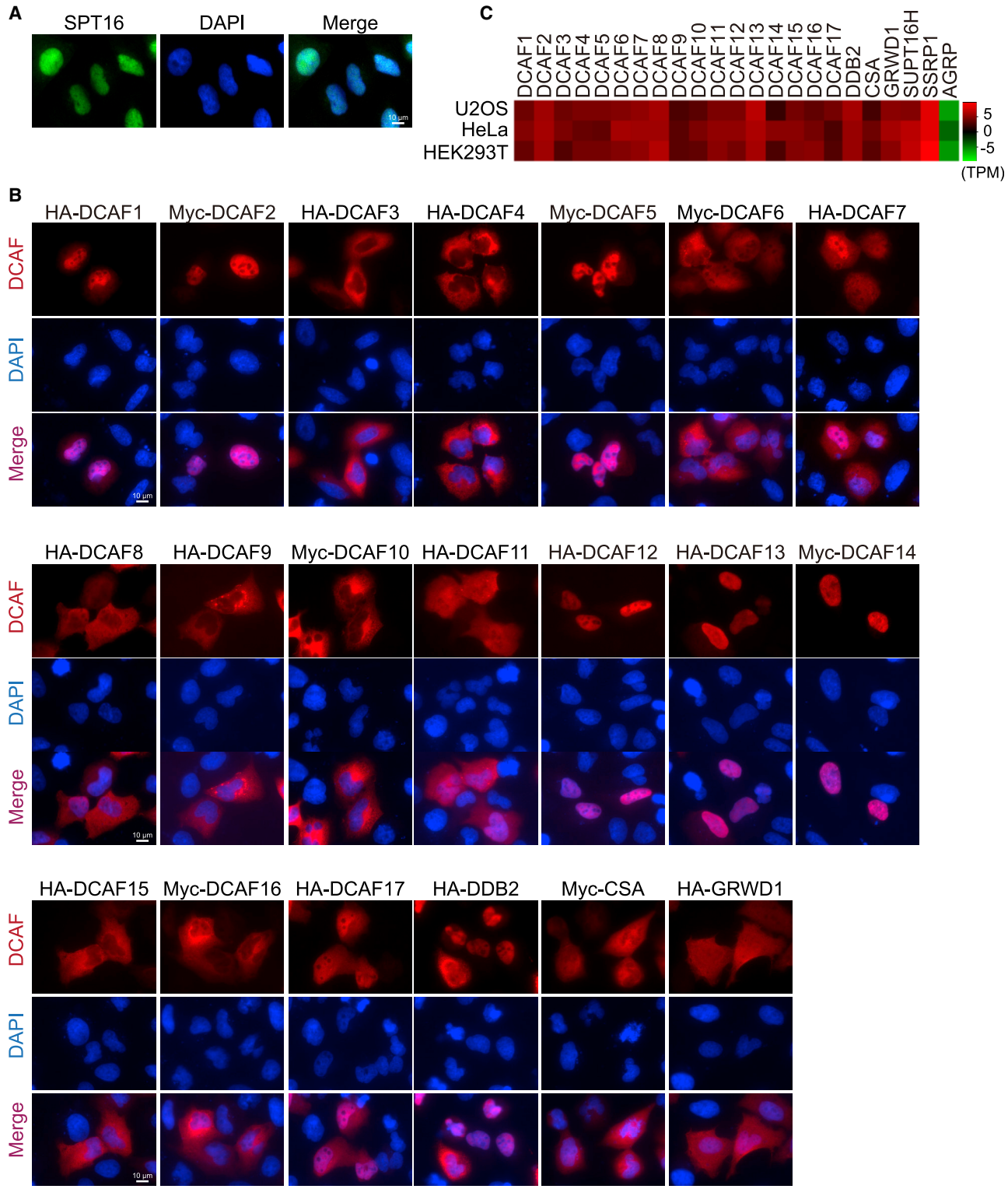

Figure 3. Subcellular localization of DCAF proteins

(A) Immunofluorescence analysis of SPT16 in U2OS cells. Nuclei were stained with DAPI. Scale bar, 10 μm. The images are representative of two independent experiments.

(B) Immunofluorescence analysis of U2OS cells expressing HA- or Myc-tagged DCAF proteins as performed with antibodies to the corresponding epitope tag. Nuclei were stained with DAPI. Scale bar, 10 μm. The images are representative of two independent experiments.

(legend continued on next page)

SPT16 and DCAF proteins localize to the nucleus

We next sought to identify DCAF proteins that link SPT16 to the CRL4 ubiquitin ligase. Given that SPT16 localizes to the nucleus (Figure 3A), we examined the subcellular localization of HA- or Myc-tagged human DCAF proteins in U2OS cells. Seven DCAF proteins (DCAF1, -2, -5, -12, 13, 14, and 17) were clearly localized to the nucleus (Figure 3B), indicating that these DCAF proteins colocalize with SPT16 at the organelle level. Examination of public transcriptomics data (Bhattacharya et al., 2021; Coronel et al., 2021; Ortmann et al., 2021) revealed that the genes for all DCAF proteins are expressed in the cell lines (U2OS, HeLa, and HEK293T) used in this study (Figures 3C and S3). These data thus implicated the identified nuclear DCAF proteins in SPT16 ubiquitylation catalyzed by the CRL4 ubiquitin ligase.

DCAF14 links SPT16 to the CRL4 ubiquitin ligase

Overexpression of various DCAF proteins in HEK293T cells revealed that forced expression of DCAF14 (also known as PHIP or BRWD2) increased the level of SPT16 ubiquitylation (Figures 4A and S1B), whereas ablation of DCAF14 with the use of the CRISPR/Cas9 system markedly attenuated SPT16 ubiquitylation (Figure 4B), indicating that DCAF14 is required for ubiquitylation of SPT16. Consistent with this conclusion, immunoprecipitation and immunoblot analyses revealed that Myc-DCAF14 interacted with FLAG-SPT16 in transfected HEK293T cells (Figure 4C). We also demonstrated the binding of SPT16 to the DCAF14-CRL4 ubiquitin ligase complex at endogenous levels of these proteins in U2OS cells (Figure S4), supporting the notion that SPT16 is a substrate of DCAF14-CRL4 in the physiological condition. The COOH-terminal portion and dimerization domain of SPT16 were found to be responsible for binding to DCAF14 (Figure 4D) as well as for that to CUL4A, CUL4B, and DDB1 (Figures 1B–1D). To map the DDB1- and SPT16-binding domains of DCAF14, we expressed full-length or NH_2-terminal (N) or COOH-terminal (C) regions of DCAF14 in HEK293T cells and examined their binding to endogenous DDB1 and SPT16. The WD40 domain—containing the NH_2-terminal region of DCAF14—was sufficient for binding to DDB1. In contrast, the bromodomain-containing COOH-terminal region was found to be responsible for association with SPT16 (Figures 4E, 4F, and S1B). Together, these results suggested that DCAF14 links SPT16 to the CRL4 ubiquitin ligase for ubiquitylation of SPT16.

Lysine-674 is a primary site of SPT16 ubiquitylation

Proteomics analysis identified 13 potential ubiquitylated lysine residues (K86, K120, K196, K426, K513, K596, K647, K663, K674, K696, K781, K786, and K904) of SPT16 in HEK293T cells (Wagner et al., 2011). However, which of these lysine residues is the primary site of SPT16 ubiquitylation is unknown. Given that SPT16 ubiquitylation is conserved from yeast to humans, we hypothesized that the primary ubiquitylation site might also be conserved. Comparison of the amino acid sequences of SPT16 and its orthologs revealed that, among the ubiquitylated lysines, only K674 of the human protein is totally conserved (Figure 5A), prompting us to examine this site further. The extent of ubiquitylation of the K674R mutant of SPT16 was markedly reduced compared with that of the WT protein in transfected HEK293T cells (Figure 5B). In contrast, the K674R substitution did not affect the binding of SPT16 to SSRP1 (Figure S5), consistent with the location of this site outside of the dimerization domain (Figure 1B). To evaluate the role of ubiquitylation of endogenous SPT16 at K674, we attempted to generate U2OS cells with the K674R substitution knocked in with the use of the CRISPR/Cas9 system (Figure 5C). Although we were not able to obtain cell clones homozygous for the K674R mutation, we did establish heterozygous knockin cells (we examined 21 clones, with 14 found to be heterozygous and 7 WT) (Figure 5D). These knockin cells manifested a greatly reduced extent of SPT16 ubiquitylation (Figure 5E), thus revealing that the K674R substitution attenuated SPT16 ubiquitylation and implicating K674 is a primary site of such ubiquitylation.

K674 ubiquitylation impairs binding of the middle domain of SPT16 to H3.1-H4

K674 is located in the middle (M) domain of SPT16 (Figure 6A). This domain of yeast Spt16 was previously shown to bind to H3.1-H4 *in vitro* (Yang et al., 2016). Mutation of K692 and R693 of Spt16 to alanine was also found to impair this association. Given that K674 of human SPT16 is equivalent to K692 of yeast Spt16, we examined the effect of K674 ubiquitylation on the binding of SPT16 to H3.1-H4. We first found that a portion of the middle domain of SPT16 (amino acids 674–933) binds to H3.1-H4 *in vitro* (Figures 6A and 6B). To mimic the ubiquitylation of SPT16 at K674, we fused ubiquitin (containing the G76A mutation to inhibit cleavage) to the NH_2 terminus of K674 in the M domain fragment of SPT16 (Figure 6A). The binding of this ubiquitin fusion protein to H3.1-H4 *in vitro* was markedly attenuated compared with that of the unmodified M domain fragment (Figure 6B), indicating that ubiquitylation of SPT16 at K674 impairs binding to H3.1-H4.

K674 is critical for DNA replication-coupled histone incorporation into chromatin

Budding yeast harboring the K692A/R693A mutant form of Spt16 manifested a reduced level of histone incorporation into chromatin during DNA replication (Yang et al., 2016). We therefore examined whether K674 ubiquitylation of SPT16 might affect histone incorporation into chromatin of HEK293T cells. Immunoblot analysis of the chromatin fraction isolated from HEK293T cells transfected with an expression vector for HA-tagged H3.1 (which is incorporated into chromatin only during DNA replication) revealed the incorporation of HA-H3.1 into chromatin (Figure 6C). Expression of the M domain fragment of SPT16 greatly attenuated such HA-H3.1 incorporation, likely as a result of sequestration of H3.1 by the M domain. However, this inhibitory effect was not observed with the ubiquitin-fused

(C) Abundance of DCAF protein, SUPT16H, SSRP1, and AGRP (neuron-specific marker examined as a negative control) mRNAs in U2OS, HeLa, and HEK293T cells (Bhattacharya et al., 2021; Coronel et al., 2021; Ortmann et al., 2021). Transcripts per million (TPM) values were log_2 transformed and then represented as a heatmap.
See also Figure S3.

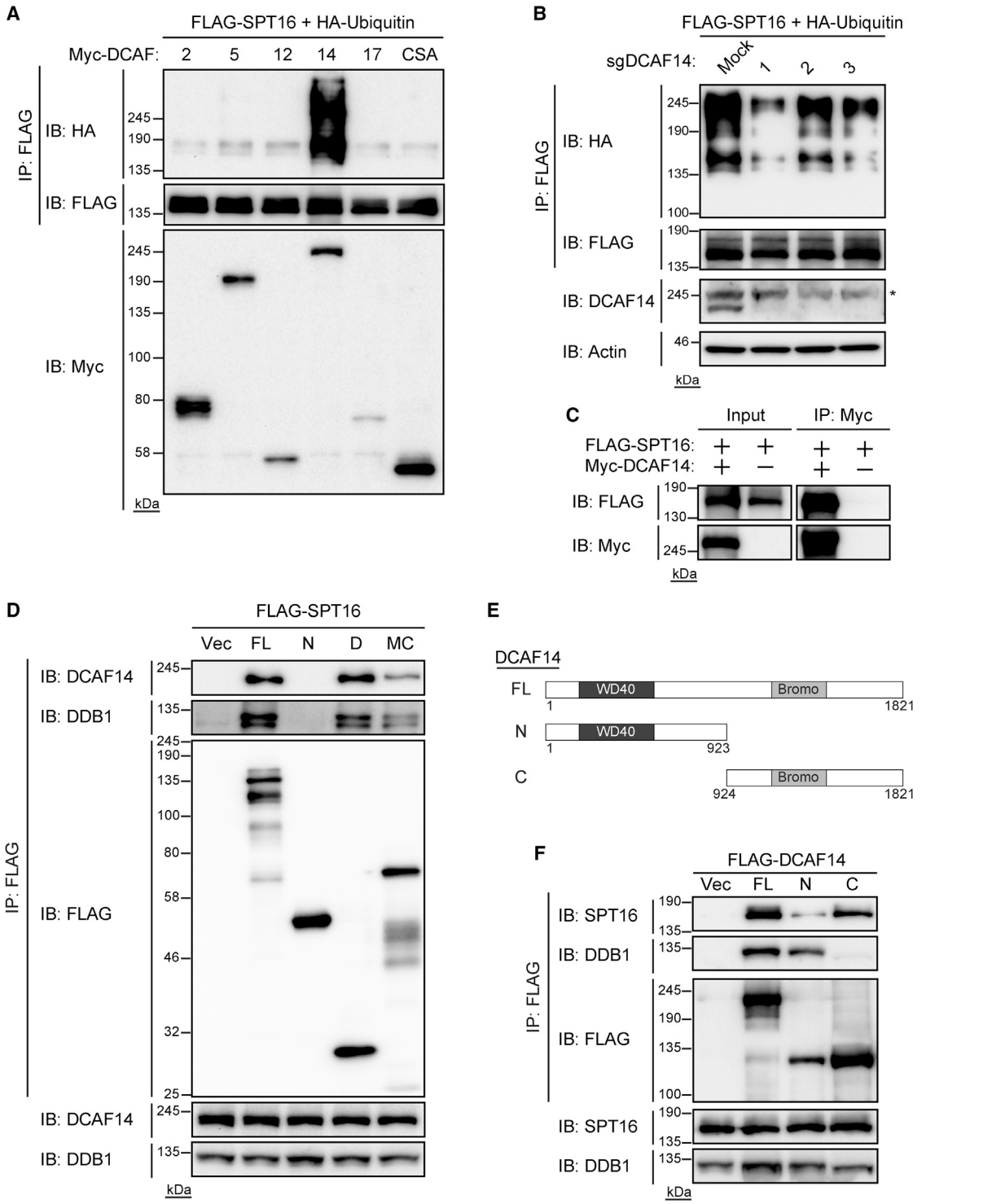

Figure 4. DCAF14 links SPT16 to the CRL4 ubiquitin ligase

(A) HEK293T cells transfected with expression plasmids for FLAG-SPT16, HA-ubiquitin, and the indicated Myc-tagged DCAF proteins were subjected to IP with antibodies to FLAG under denaturing conditions. The resulting precipitates as well as the original cell lysates were then subjected to IB analysis with the indicated antibodies. The images are representative of two independent experiments.

(B) HEK293T cells transfected with CRISPR/Cas9 vectors targeting three different regions of exon 1 of the DCAF14 gene (sgDCAF14) were subjected to selection with puromycin (2 μg/mL) for 3 days and then transfected with expression plasmids for FLAG-SPT16 and HA-ubiquitin. Cell lysates were subjected to IP with

(legend continued on next page)

M domain fragment, suggesting that ubiquitylation of SPT16 at K674 regulates H3.1 incorporation into chromatin. Consistent with this finding, expression of the K674R mutant of SPT16, but not that of the WT protein, reduced the amount of HA-H3.1 in the chromatin fraction of transfected HEK293T cells (Figure 6D). Furthermore, U2OS cells heterozygous for the K674R substitution of SPT16 also manifested a reduced level of HA-H3.1 incorporation into chromatin compared with parental cells (Figure 6E). We also detected enhanced binding of the nonubiquitylatable (K674R) form of SPT16 to histone H3.1 (Figure 6F) but not to H2A (Figure S6). Collectively, these results supported the notion that K674 ubiquitylation of SPT16 regulates DNA replication-coupled histone incorporation into chromatin by promoting histone release from SPT16.

K674 ubiquitylation of SPT16 is related to resistance to DNA replication stress

The ubiquitylation of SPT16 and the DNA replication-coupled histone incorporation into chromatin mediated by SPT16 prompted us to determine when during the cell cycle SPT16 is ubiquitylated. HeLa cells transfected with expression vectors for FLAG-SPT16 and HA-ubiquitin were synchronized by treatment either with thymidine to arrest cells at S phase or with nocodazole to induce M phase arrest, and cell extracts were then examined for SPT16 ubiquitylation. We found that the level of SPT16 ubiquitylation was high in S phase but almost undetectable in M phase (Figure 7A), consistent with a role for such ubiquitylation in DNA replication-coupled histone incorporation into chromatin. In contrast, the ubiquitylation level of SPT16 in HEK293T cells was not altered by inhibition of transcription with actinomycin D (Figures S7A and S7B), suggesting that SPT16 ubiquitylation does not play a substantial role in the transcription process. We then investigated the effect of SPT16 ubiquitylation on cell cycle progression. Flow cytometric analysis revealed that heterozygous knockin of the K674R mutant form of SPT16 in U2OS cells increased the proportion of cells in mid S phase, but not that of those in early or late S phase (Figures 7B, S7C, and S7D), and that this effect was associated with a significant slowdown of cell proliferation (Figure 7C), indicating that SPT16 ubiquitylation at K674 is important for DNA replication. Finally, we examined whether tolerance to S-phase stress might be related to proper chromatin assembly dependent on SPT16 ubiquitylation. We thus treated parental or +/*K674R* lines of U2OS cells with hydroxyurea (HU) and then examined colony formation. Significantly fewer +/*K674R* cells survived HU-induced stress compared with parental cells (Figure 7D). DNA replication stress induces DNA double-strand breaks that are associated with phosphorylated H2AX (γH2AX) (Burdova et al., 2019), and we found that the HU-induced increase in γH2AX level was significantly greater in +/*K674R* U2OS cells than in parental cells (Figure 7E). Of note, K692A/R693A mutation of Spt16 in budding yeast was also found to increase sensitivity to HU-induced cell death (Yang et al., 2016). Our results thus suggested that SPT16 ubiquitylation is critical for S phase progression and resistance to replication stress (Figure 7F).

DISCUSSION

Regulation of chromatin structure is key to DNA-based processes such as gene transcription, genome replication and repair, and chromosome segregation, and specific histone chaperones play a role in each of these processes (Burgess and Zhang, 2013; Gurard-Levin et al., 2014; Hammond et al., 2017). However, one such chaperone, FACT, plays a role not only in transcription, for which it was originally identified, but also in DNA replication and repair (Gurova et al., 2018; Winkler and Luger, 2011). How FACT is directed to regulate a specific process and how its functions are controlled have remained unknown, however. We have now shown that SPT16 is ubiquitylated at K674 by a DCAF14-linked CRL4 ubiquitin ligase in S phase of the cell cycle in mammalian cells and that this ubiquitylation may regulate histone incorporation into newly synthesized DNA by promoting histone release from the chaperone, ensuring efficient progression of S phase.

We found that K674 ubiquitylation regulates SPT16-dependent histone incorporation only during S phase, indicating that other mechanisms might operate to induce histone release by FACT in other phases of the cell cycle and other cellular processes. Consistent with this possibility, we did not detect a notable difference in the level of SPT16 ubiquitylation during transcriptional stress. The notion that CRL4-mediated ubiquitylation of SPT16 reduces FACT association with H3-H4 is reminiscent of histone handoff by ASF1, which is also regulated by CRL4-dependent ubiquitylation. ASF1 is also an H3-H4 chaperone but is dedicated to DNA replication-coupled histone incorporation (Han et al., 2013). Whether or how FACT and ASF1 interact in the process of nucleosome assembly after DNA replication remains unknown. Determination of whether ASF1 and

antibodies to FLAG under denaturing conditions, and the resulting precipitates as well as the original cell lysates were subjected to IB analysis with the indicated antibodies. Actin was examined as a loading control. The asterisk indicates nonspecific bands. The images are representative of two independent experiments.
(C) HEK293T cells transfected with expression plasmids for FLAG-SPT16 and Myc-DCAF14 were subjected to IP with antibodies to Myc, and the resulting precipitates as well as the original cell lysates (Input) were subjected to IB analysis with antibodies to FLAG and to Myc. The images are representative of two independent experiments.
(D) HEK293T cells transfected with expression plasmids for FLAG-tagged FL or mutant forms of SPT16 (Figure 1B), or with the corresponding empty vector (Vec), were subjected to IP with antibodies to FLAG, and the resulting precipitates as well as the original cell lysates were subjected to IB analysis with the indicated antibodies. The images are representative of two independent experiments.
(E) Domain structure of FL human DCAF14 as well as the structure of NH_2-terminal (N, amino acids 1–923) and COOH-terminal (C, amino acids 924–1821) portions of the protein examined in (F). WD40, WD40 domain; Bromo, bromodomain.
(F) HEK293T cells transfected with expression plasmids for FLAG-tagged FL, N, or C forms of DCAF14 were subjected to IP with antibodies to FLAG, and the resulting precipitates as well as the original cell lysates were subjected to IB analysis with the indicated antibodies. The images are representative of two independent experiments.
See also Figures S1 and S4.

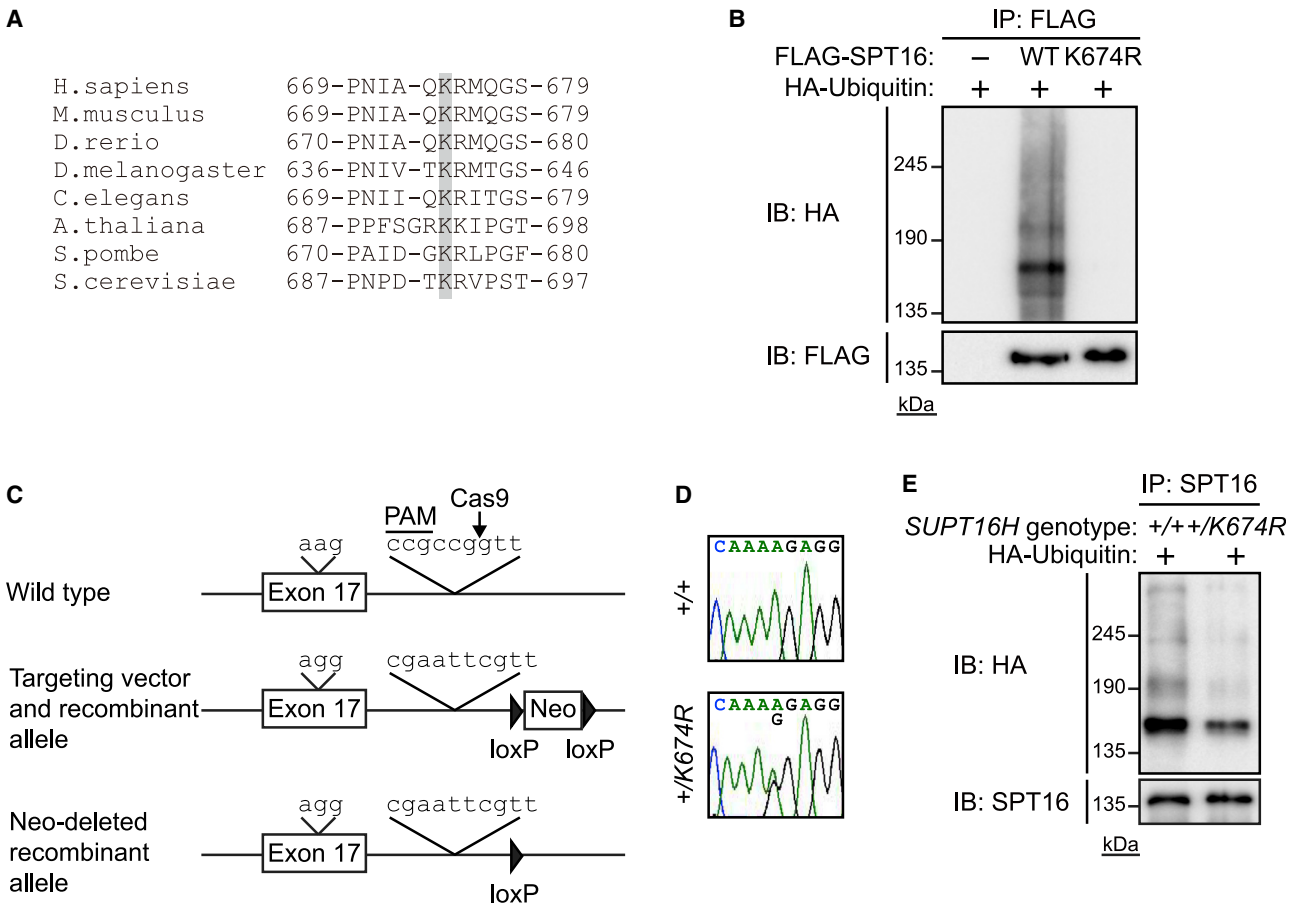

Figure 5. Lysine-674 is a primary site of SPT16 ubiquitylation

(A) Amino acid sequences of SPT16 orthologs corresponding to the region surrounding lysine-674 (shaded) of the human protein as retrieved from the NCBI database (https://www.ncbi.nlm.nih.gov/homologene/5207). Species are *Homo sapiens*, *Mus musculus*, *Danio rerio*, *Drosophila melanogaster*, *Caenorhabditis elegans*, *Arabidopsis thaliana*, *Schizosaccharomyces pombe*, and *Saccharomyces cerevisiae*.

(B) HEK293T cells transfected with expression plasmids for HA-ubiquitin and FLAG-tagged WT or K674R mutant forms of SPT16 were subjected to IP with antibodies to FLAG under denaturing conditions, and the resulting precipitates were subjected to IB analysis with antibodies to HA and to FLAG. The images are representative of two independent experiments.

(C) Schematic representation of the knockin strategy for establishment of U2OS cells expressing the K674R mutant of SPT16, with the critical bases indicated. PAM, protospacer adjacent motif; Neo, neomycin resistance gene.

(D) Sanger sequencing of genomic DNA extracted from parental (+/+) U2OS cells and from cells heterozygous for knockin of the K674R mutation of SPT16 (+/*K674R*).

(E) Parental or SPT16(K674R) knockin U2OS cells transfected with an expression plasmid for HA-ubiquitin were subjected to IP with antibodies to SPT16 under denaturing conditions. The resulting precipitates were subjected to IB analysis with antibodies to HA and to SPT16. The images are representative of two independent experiments.

See also Figure S5.

SPT16 share the same substrate receptor (DCAF14) for CRL4-dependent ubiquitylation should provide further insight into their relative roles in histone incorporation and DNA replication.

We identified DCAF14 as the link between SPT16 and the catalytic module of the CRL4 ubiquitin ligase complex. However, the molecular mechanism by which DCAF14 targets SPT16 for ubiquitylation specifically in S phase remains unclear. The previous finding that DCAF14 is recruited to chromatin in early S phase (Jang et al., 2018) suggests that recruitment of SPT16 to chromatin may determine its ubiquitylation. Given our finding that SPT16 binds to the COOH-terminal region of DCAF14 containing the bromodomain, it is also possible that posttranslational modification of SPT16—such as by acetylation, with the bromodomain having been shown to bind to acetylated residues (Fujisawa and Filippakopoulos, 2017)—determines its susceptibility to ubiquitylation.

In support of a role for SPT16 ubiquitylation in efficient DNA replication, we observed that susceptibility to DNA replication stress was increased in cells heterozygous for the K674R substitution of SPT16. Replication stress is defined as the slowing or stalling of replication fork progression or of DNA synthesis (Zeman and Cimprich, 2014). Although the mechanism by which the loss of SPT16 ubiquitylation reduces cellular tolerance to DNA replication stress remains unknown, we speculate that

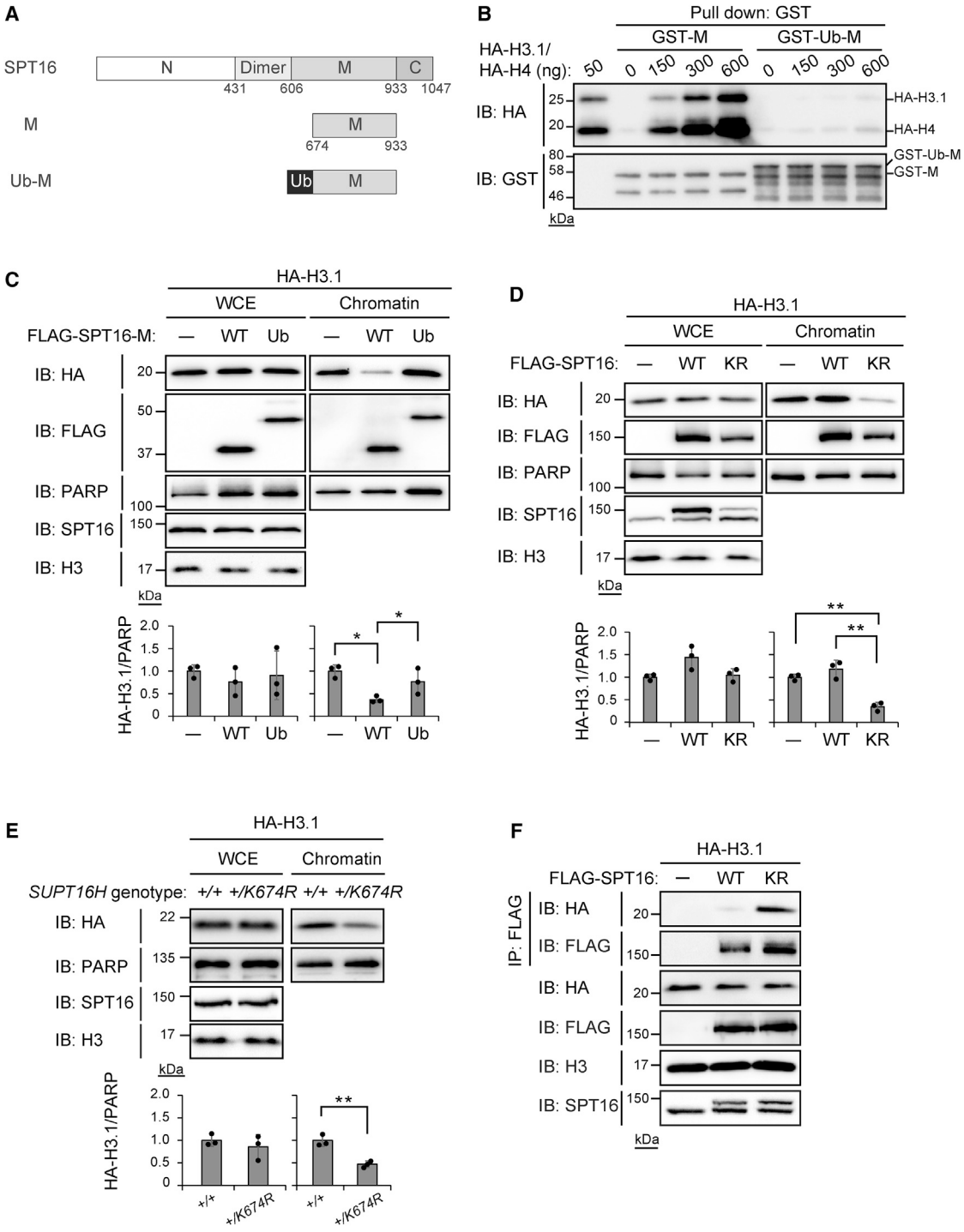

Figure 6. K674 ubiquitylation impairs binding of the middle domain of SPT16 to H3.1-H4 and promotes histone incorporation into chromatin

(A) Domain structure of full-length human SPT16 as well as the structure of M domain and ubiquitin (Ub)-fused M domain fragments examined in (B and C).

(B) Glutathione S-transferase (GST)-tagged forms of the M domain fragment (GST-M) or the ubiquitin-fused M domain fragment (GST-Ub-M) of SPT16 were bound to glutathione beads and incubated with the indicated amounts of HA-tagged histone H3.1 and H4. The precipitated proteins (Pull-down) were then subjected to IB analysis with antibodies to HA and to GST. Full-length protein bands are indicated to distinguish them from those corresponding to their degradation products. The images are representative of two independent experiments.

(C) Whole cell extracts (WCEs) or purified chromatin fractions were prepared from HEK293T cells transfected with expression plasmids for HA-H3.1 and FLAG-tagged forms of the M domain fragment of SPT16 (WT or Ub fused). Both sample types were then subjected to IB analysis with antibodies to HA, to FLAG, to

(legend continued on next page)

recovery from the slowing or stalling of replication fork progression might be mediated by histone incorporation that is dependent on SPT16 ubiquitylation. Further study is necessary to validate this hypothesis and may shed light on a possible contribution of SPT16 ubiquitylation to DNA repair processes.

Heterozygous loss-of-function mutations of *DCAF14* have been identified in individuals with neurodevelopmental disorders (Craddock et al., 2019; de Ligt et al., 2012; Jansen et al., 2018; Wang et al., 2016; Webster et al., 2016). Given that such disorders are thought to be caused by embryonic or perinatal abnormalities of neural lineage development, it is possible that mutation of *DCAF14* induces aberrant proliferation of neural stem cells through impairment of S phase progression—as was recently shown for *Setd5* mutation (Nakagawa et al., 2020)—with such impairment being due to dysfunction of SPT16. This hypothesis is supported by the identification of heterozygous loss-of-function mutations of *DDB1* (White et al., 2021), loss-of-function mutations of the X-linked gene *CUL4B* in males (Badura-Stronka et al., 2010; Isidor et al., 2010; Lopez et al., 2020; Tarpey et al., 2007; Zou et al., 2007), and missense and deletion mutations of *SUPT16H* (the gene encoding SPT16) (Bina et al., 2020) among individuals with neurodevelopmental disorders.

Finally, in contrast to yeast Pob3, our ubiquitylation assay revealed that SSRP1 is also ubiquitylated. Functional characterization of this modification may provide insight into regulation of the different aspects of FACT function in DNA-related processes as well as into why FACT functions as a dimer in mammals and a trimer in yeast. Identification of the ubiquitin ligase that targets SSRP1 will be a key step of such a study, with DCAF14-CRL4 being a potential candidate on the basis of our observation that it binds not only to the COOH-terminal region but also to the dimerization domain of SPT16.

Limitations of the study

We found that inhibition of transcription did not affect SPT16 ubiquitylation. However, this finding does not necessarily demonstrate that ubiquitylation of FACT specifically controls replication-dependent histone incorporation into chromatin. The time resolution of our experiments was not sufficient to determine whether histones fail to incorporate into or are lost from chromatin once incorporated in cells in which SPT16 ubiquitylation is inhibited, although our biochemical data showing that SPT16 ubiquitylation attenuates histone binding support the former possibility. Experiments based on overexpression of SPT16 also might influence H3.1 availability for deposition without reflecting a normal function of FACT. Given that we were not able to generate cells homozygous for the K674R mutation of SPT16, we could not definitively show that K674 ubiquitylation of SPT16 is essential for replication-coupled incorporation of histone H3.1 into chromatin and consequent efficient progression of S phase. In addition, our study was based on cultured cancer cell lines, with the consequence that our finding that SPT16 ubiquitylation plays a role in DNA replication was not validated *in vivo*.

STAR★METHODS

Detailed methods are provided in the online version of this paper and include the following:

- KEY RESOURCES TABLE
- RESOURCE AVAILABILITY
  - Lead contact
  - Materials availability
  - Data and code availability
- EXPERIMENTAL MODEL AND SUBJECT DETAILS
  - Cell culture
- METHOD DETAILS
  - Plasmid construction
  - Immunoprecipitation
  - Ubiquitylation assay
  - RNA interference
  - *In vitro* binding assay
  - Immunofluorescence staining
  - Generation of SPT16(K674R) knockin cells
  - Chromatin fractionation
  - Colony formation assay
  - Cell counting
  - Flow cytometry
  - Analysis of transcriptomics data
- QUANTIFICATION AND STATISTICAL ANALYSIS

SUPPLEMENTAL INFORMATION

Supplemental information can be found online at https://doi.org/10.1016/j.celrep.2022.110541.

ACKNOWLEDGMENTS

We thank laboratory members for discussion as well as the Biomedical Research Core of Tohoku University Graduate School of Medicine for technical support. This work was funded by KAKENHI grants 19K07837 (T.N.) and 21H02458 (K.N.) from the Japan Society for the Promotion of Science.

poly(ADP-ribose) polymerase (PARP, loading control), to SPT16, or to H3. The relative HA-H3.1/PARP band intensity ratio was determined by densitometry, and the quantitative data are means ± SD (n = 3 independent experiments). *p < 0.05 (one-way ANOVA followed by Tukey's test).

(D) WCEs or purified chromatin fractions prepared from HEK293T cells transfected with expression plasmids for HA-H3.1 and FLAG–SPT16 (WT or K674R) were subjected to IB analysis with the indicated antibodies. The relative HA-H3.1/PARP band intensity ratio was determined by densitometry, and the quantitative data are means ± SD (n = 3 independent experiments). **p < 0.01 (one-way ANOVA followed by Tukey's test).

(E) WCEs or purified chromatin fractions prepared from parental (+/+) or SPT16(K674R) knockin (+/*K674R*) U2OS cells transfected with an expression plasmid for HA-H3.1 were subjected to IB analysis with the indicated antibodies. The relative HA-H3.1/PARP band intensity ratio was determined by densitometry, and the quantitative data are means ± SD (n = 3 independent experiments). **p < 0.01 (unpaired two-tailed Student's *t* test).

(F) The chromatin fraction of HEK293T cells transfected with an expression plasmid for HA-H3.1 was mixed with lysates of HEK293T cells transfected with a vector for FLAG–SPT16 (WT or K674R mutant), and the mixtures were subjected to IP with antibodies to FLAG. The resulting precipitates as well as the original mixtures were subjected to IB analysis with the indicated antibodies. The images are representative of two independent experiments.

See also Figure S6.

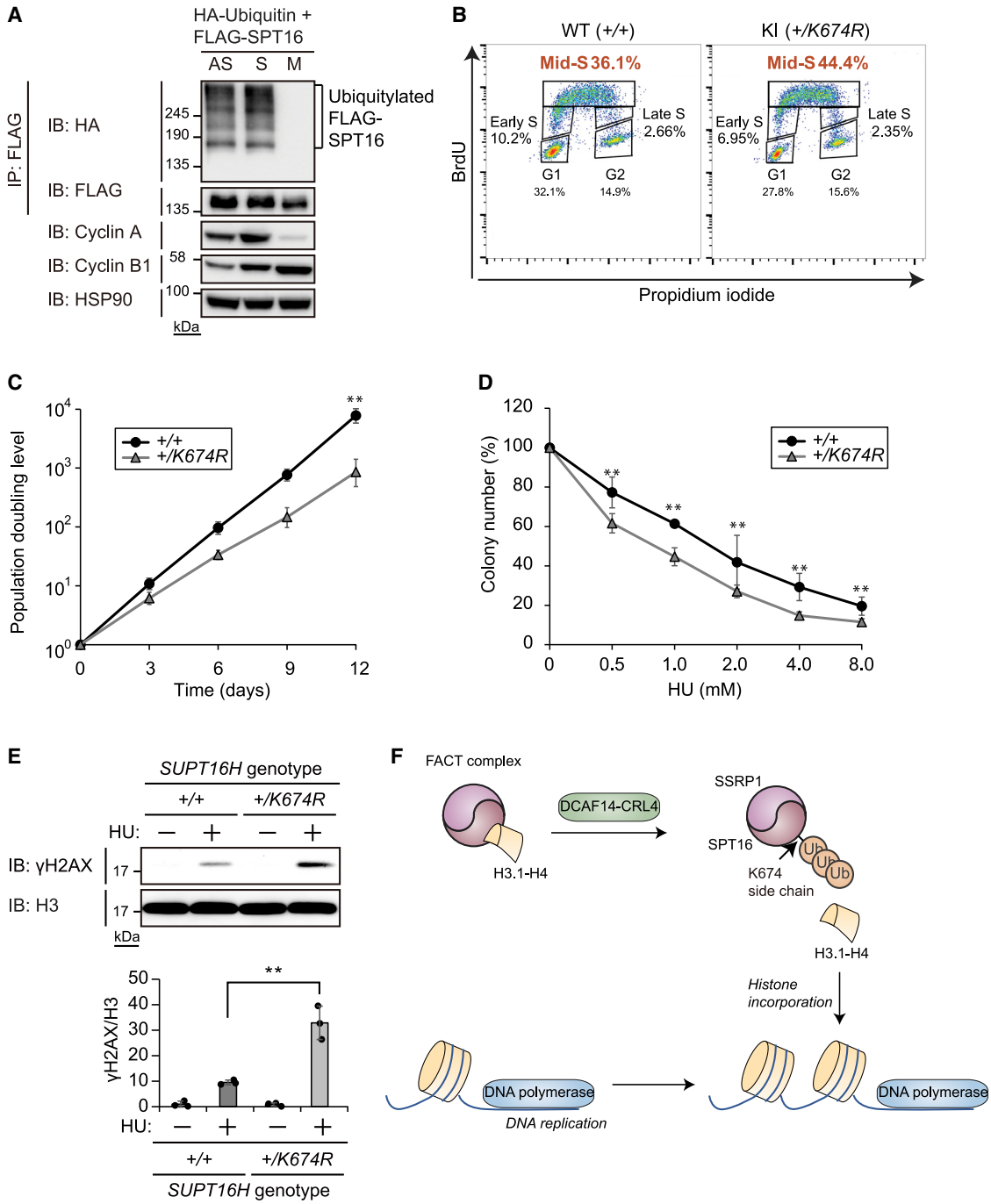

Figure 7. K674 ubiquitylation of SPT16 is related to S phase progression and resistance to DNA replication stress

(A) HeLa cells transfected with expression plasmids for FLAG-SPT16 and HA-ubiquitin were synchronized at S phase with thymidine or at M phase with nocodazole and were then subjected to IP with antibodies to FLAG under denaturing conditions. The resulting precipitates as well as the original cell lysates were subjected to IB analysis with the indicated antibodies. Asynchronous (AS) cells were similarly analyzed. Cyclin A served as an S phase marker and cyclin B1 as an M phase marker. The images are representative of two independent experiments.

(B) Flow cytometric analysis of cell cycle distribution for parental (+/+) and SPT16(K674R) knockin (KI; +/*K674R*) U2OS cells stained for incorporated bromodeoxyuridine (BrdU) and with propidium iodide. The images are representative of four independent experiments.

(C) Cumulative cell number for parental (+/+) and SPT16(K674R) knockin (+/*K674R*) U2OS cells. Data are means ± SD (n = 4 independent experiments). **p < 0.01 versus the corresponding value for the mutant cells (two-way ANOVA followed by Tukey's test).

(D) Parental (+/+) or SPT16(K674R) knockin (+/*K674R*) U2OS cells were treated with the indicated concentrations of HU for 24 h and then incubated in the absence of HU for an additional 14 days. They were then stained with Giemsa solution for quantitation of colony formation. Data are means ± SD (n = 3 independent experiments). **p < 0.01 versus the corresponding value for the mutant cells (two-way ANOVA followed by Tukey's test).

(legend continued on next page)

AUTHOR CONTRIBUTIONS

T.N., A.M., and K.N. designed the research plan. T.N., A.M., Y. Nagasawa, and M.N. performed experiments. M.H., Y. Noda, and T.H. provided advice. T.N. and K.N. wrote and edited the manuscript.

DECLARATION OF INTERESTS

The authors declare no competing interests.

Received: August 27, 2021
Revised: December 23, 2021
Accepted: February 28, 2022
Published: March 22, 2022

REFERENCES

Akutsu, M., Dikic, I., and Bremm, A. (2016). Ubiquitin chain diversity at a glance. J. Cell Sci. *129*, 875–880.

Badura-Stronka, M., Jamsheer, A., Materna-Kiryluk, A., Sowinska, A., Kiryluk, K., Budny, B., and Latos-Bielenska, A. (2010). A novel nonsense mutation in CUL4B gene in three brothers with X-linked mental retardation syndrome. Clin. Genet. *77*, 141–144.

Bannister, A.J., and Kouzarides, T. (2011). Regulation of chromatin by histone modifications. Cell Res. *21*, 381–395.

Bhattacharya, S., Levy, M.J., Zhang, N., Li, H., Florens, L., Washburn, M.P., and Workman, J.L. (2021). The methyltransferase SETD2 couples transcription and splicing by engaging mRNA processing factors through its SHI domain. Nat. Commun. *12*, 1443.

Bina, R., Matalon, D., Fregeau, B., Tarsitano, J.J., Aukrust, I., Houge, G., Bend, R., Warren, H., Stevenson, R.E., Stuurman, K.E., et al. (2020). De novo variants in SUPT16H cause neurodevelopmental disorders associated with corpus callosum abnormalities. J. Med. Genet. *57*, 461–465.

Burdova, K., Yang, H., Faedda, R., Hume, S., Chauhan, J., Ebner, D., Kessler, B.M., Vendrell, I., Drewry, D.H., Wells, C.I., et al. (2019). E2F1 proteolysis via SCF-cyclin F underlies synthetic lethality between cyclin F loss and Chk1 inhibition. EMBO J. *38*, e101443.

Burgess, R.J., and Zhang, Z. (2013). Histone chaperones in nucleosome assembly and human disease. Nat. Struct. Mol. Biol. *20*, 14–22.

Clapier, C.R., Iwasa, J., Cairns, B.R., and Peterson, C.L. (2017). Mechanisms of action and regulation of ATP-dependent chromatin-remodelling complexes. Nat. Rev. Mol. Cell Biol. *18*, 407–422.

Coronel, L., Riege, K., Schwab, K., Forste, S., Hackes, D., Semerau, L., Bernhart, S.H., Siebert, R., Hoffmann, S., and Fischer, M. (2021). Transcription factor RFX7 governs a tumor suppressor network in response to p53 and stress. Nucleic Acids Res. *49*, 7437–7456.

Craddock, K.E., Okur, V., Wilson, A., Gerkes, E.H., Ramsey, K., Heeley, J.M., Juusola, J., Vitobello, A., Dupeyron, M.B., Faivre, L., et al. (2019). Clinical and genetic characterization of individuals with predicted deleterious PHIP variants. Cold Spring Harb. Mol. Case Stud. *5*, a004200.

de Ligt, J., Willemsen, M.H., van Bon, B.W., Kleefstra, T., Yntema, H.G., Kroes, T., Vulto-van Silfhout, A.T., Koolen, D.A., de Vries, P., Gilissen, C., et al. (2012). Diagnostic exome sequencing in persons with severe intellectual disability. N. Engl. J. Med. *367*, 1921–1929.

Deshaies, R.J., and Joazeiro, C.A. (2009). RING domain E3 ubiquitin ligases. Annu. Rev. Biochem. *78*, 399–434.

Fujisawa, T., and Filippakopoulos, P. (2017). Functions of bromodomain-containing proteins and their roles in homeostasis and cancer. Nat. Rev. Mol. Cell Biol. *18*, 246–262.

Funayama, R., Taniguchi, H., Mizuma, M., Fujishima, F., Kobayashi, M., Ohnuma, S., Unno, M., and Nakayama, K. (2017). Protein-arginine deiminase 2 suppresses proliferation of colon cancer cells through protein citrullination. Cancer Sci. *108*, 713–718.

Glickman, M.H., and Ciechanover, A. (2002). The ubiquitin-proteasome proteolytic pathway: destruction for the sake of construction. Physiol. Rev. *82*, 373–428.

Greenberg, M.V.C., and Bourc'his, D. (2019). The diverse roles of DNA methylation in mammalian development and disease. Nat. Rev. Mol. Cell Biol. *20*, 590–607.

Gurard-Levin, Z.A., Quivy, J.P., and Almouzni, G. (2014). Histone chaperones: assisting histone traffic and nucleosome dynamics. Annu. Rev. Biochem. *83*, 487–517.

Gurova, K., Chang, H.W., Valieva, M.E., Sandlesh, P., and Studitsky, V.M. (2018). Structure and function of the histone chaperone FACT—resolving FACTual issues. Biochim. Biophys. Acta Gene Regul. Mech. *1861*, 892–904.

Hammond, C.M., Stromme, C.B., Huang, H., Patel, D.J., and Groth, A. (2017). Histone chaperone networks shaping chromatin function. Nat. Rev. Mol. Cell Biol. *18*, 141–158.

Han, J., Li, Q., McCullough, L., Kettelkamp, C., Formosa, T., and Zhang, Z. (2010). Ubiquitylation of FACT by the cullin-E3 ligase Rtt101 connects FACT to DNA replication. Genes Dev. *24*, 1485–1490.

Han, J., Zhang, H., Zhang, H., Wang, Z., Zhou, H., and Zhang, Z. (2013). A Cul4 E3 ubiquitin ligase regulates histone hand-off during nucleosome assembly. Cell *155*, 817–829.

Hannah, J., and Zhou, P. (2015). Distinct and overlapping functions of the cullin E3 ligase scaffolding proteins CUL4A and CUL4B. Gene *573*, 33–45.

Hershko, A., and Ciechanover, A. (1998). The ubiquitin system. Annu. Rev. Biochem. *67*, 425–479.

Ishida, N., Nakagawa, T., Iemura, S.I., Yasui, A., Shima, H., Katoh, Y., Nagasawa, Y., Natsume, T., Igarashi, K., and Nakayama, K. (2017). Ubiquitylation of Ku80 by RNF126 promotes completion of nonhomologous end joining-mediated DNA repair. Mol. Cell. Biol. *37*, e00347.

Isidor, B., Pichon, O., Baron, S., David, A., and Le Caignec, C. (2010). Deletion of the CUL4B gene in a boy with mental retardation, minor facial anomalies, short stature, hypogonadism, and ataxia. Am. J. Med. Genet. *152A*, 175–180.

Jackson, S., and Xiong, Y. (2009). CRL4s: the CUL4-RING E3 ubiquitin ligases. Trends Biochem. Sci. *34*, 562–570.

Jang, S.M., Zhang, Y., Utani, K., Fu, H., Redon, C.E., Marks, A.B., Smith, O.K., Redmond, C.J., Baris, A.M., Tulchinsky, D.A., et al. (2018). The replication initiation determinant protein (RepID) modulates replication by recruiting CUL4 to chromatin. Nat. Commun. *9*, 2782.

Jansen, S., Hoischen, A., Coe, B.P., Carvill, G.L., Van Esch, H., Bosch, D.G.M., Andersen, U.A., Baker, C., Bauters, M., Bernier, R.A., et al. (2018). A genotype-first approach identifies an intellectual disability-overweight syndrome caused by PHIP haploinsufficiency. Eur. J. Hum. Genet. *26*, 54–63.

Lopez, M., Perez-Grijalba, V., Garcia-Cobaleda, I., and Dominguez-Garrido, E. (2020). A 22.5 kb deletion in CUL4B causing Cabezas syndrome identified using CNV approach from WES data. Clin. Case Rep. *8*, 3184–3188.

Luger, K., Mader, A.W., Richmond, R.K., Sargent, D.F., and Richmond, T.J. (1997). Crystal structure of the nucleosome core particle at 2.8 A resolution. Nature *389*, 251–260.

(E) Parental (+/+) or SPT16(K674R) knockin (+/*K674R*) U2OS cells were incubated in the absence or presence of 2 mM HU for 30 min, after which the chromatin fraction was purified and subjected to IB analysis with the indicated antibodies. The relative γH2AX/H3 band intensity ratio was determined by densitometry, and the quantitative data are means ± SD (n = 3 independent experiments). **$p < 0.01$ (one-way ANOVA followed by Tukey's test).
(F) Model for the role of SPT16 ubiquitylation at K674 by DCAF14-CRL4 in H3.1-H4 incorporation into chromatin during DNA replication. See text for further details.
See also Figure S7.

Martire, S., and Banaszynski, L.A. (2020). The roles of histone variants in fine-tuning chromatin organization and function. Nat. Rev. Mol. Cell Biol. *21*, 522–541.

Mendez, J., and Stillman, B. (2000). Chromatin association of human origin recognition complex, cdc6, and minichromosome maintenance proteins during the cell cycle: assembly of prereplication complexes in late mitosis. Mol. Cell. Biol. *20*, 8602–8612.

Metzger, M.B., Hristova, V.A., and Weissman, A.M. (2012). HECT and RING finger families of E3 ubiquitin ligases at a glance. J. Cell Sci. *125*, 531–537.

Naito, Y., Hino, K., Bono, H., and Ui-Tei, K. (2015). CRISPRdirect: software for designing CRISPR/Cas guide RNA with reduced off-target sites. Bioinformatics *31*, 1120–1123.

Nakagawa, T., Hattori, S., Nobuta, R., Kimura, R., Nakagawa, M., Matsumoto, M., Nagasawa, Y., Funayama, R., Miyakawa, T., Inada, T., et al. (2020). The autism-related protein SETD5 controls neural cell proliferation through epigenetic regulation of rDNA expression. iScience *23*, 101030.

Nakagawa, T., Hosogane, M., Nakagawa, M., Morohoshi, A., Funayama, R., and Nakayama, K. (2018). Transforming growth factor β-induced proliferative arrest mediated by TRIM26-dependent TAF7 degradation and its antagonism by MYC. Mol. Cell. Biol. *38*, e00449.

Nakagawa, T., Lv, L., Nakagawa, M., Yu, Y., Yu, C., D'Alessio, A.C., Nakayama, K., Fan, H.Y., Chen, X., and Xiong, Y. (2015). CRL4(VprBP) E3 ligase promotes monoubiquitylation and chromatin binding of TET dioxygenases. Mol. Cell *57*, 247–260.

Nakagawa, T., and Nakayama, K. (2015). Protein monoubiquitylation: targets and diverse functions. Genes Cells *20*, 543–562.

Nakagawa, T., and Xiong, Y. (2011). X-linked mental retardation gene CUL4B targets ubiquitylation of H3K4 methyltransferase component WDR5 and regulates neuronal gene expression. Mol. Cell *43*, 381–391.

Nakayama, K.I., and Nakayama, K. (2006). Ubiquitin ligases: cell-cycle control and cancer. Nat. Rev. Cancer *6*, 369–381.

Orphanides, G., LeRoy, G., Chang, C.H., Luse, D.S., and Reinberg, D. (1998). FACT, a factor that facilitates transcript elongation through nucleosomes. Cell *92*, 105–116.

Ortmann, B.M., Burrows, N., Lobb, I.T., Arnaiz, E., Wit, N., Bailey, P.S.J., Jordon, L.H., Lombardi, O., Penalver, A., McCaffrey, J., et al. (2021). The HIF complex recruits the histone methyltransferase SET1B to activate specific hypoxia-inducible genes. Nat. Genet. *53*, 1022–1035.

Petroski, M.D., and Deshaies, R.J. (2005). Function and regulation of cullin-RING ubiquitin ligases. Nat. Rev. Mol. Cell Biol. *6*, 9–20.

Prieto, C., and Barrios, D. (2019). RaNA-Seq: interactive RNA-Seq analysis from FASTQ files to functional analysis. Bioinformatics *36*, 1955–1956.

Ran, F.A., Hsu, P.D., Wright, J., Agarwala, V., Scott, D.A., and Zhang, F. (2013). Genome engineering using the CRISPR-Cas9 system. Nat. Protoc. *8*, 2281–2308.

Rotin, D., and Kumar, S. (2009). Physiological functions of the HECT family of ubiquitin ligases. Nat. Rev. Mol. Cell Biol. *10*, 398–409.

Sarikas, A., Hartmann, T., and Pan, Z.Q. (2011). The cullin protein family. Genome Biol. *12*, 220.

Swatek, K.N., and Komander, D. (2016). Ubiquitin modifications. Cell Res. *26*, 399–422.

Tarpey, P.S., Raymond, F.L., O'Meara, S., Edkins, S., Teague, J., Butler, A., Dicks, E., Stevens, C., Tofts, C., Avis, T., et al. (2007). Mutations in CUL4B, which encodes a ubiquitin E3 ligase subunit, cause an X-linked mental retardation syndrome associated with aggressive outbursts, seizures, relative macrocephaly, central obesity, hypogonadism, pes cavus, and tremor. Am. J. Hum. Genet. *80*, 345–352.

Wagner, S.A., Beli, P., Weinert, B.T., Nielsen, M.L., Cox, J., Mann, M., and Choudhary, C. (2011). A proteome-wide, quantitative survey of in vivo ubiquitylation sites reveals widespread regulatory roles. Mol. Cell. Proteomics *10*, M111.013284.

Wang, T., Guo, H., Xiong, B., Stessman, H.A., Wu, H., Coe, B.P., Turner, T.N., Liu, Y., Zhao, W., Hoekzema, K., et al. (2016). De novo genic mutations among a Chinese autism spectrum disorder cohort. Nat. Commun. *7*, 13316.

Webster, E., Cho, M.T., Alexander, N., Desai, S., Naidu, S., Bekheirnia, M.R., Lewis, A., Retterer, K., Juusola, J., and Chung, W.K. (2016). De novo PHIP-predicted deleterious variants are associated with developmental delay, intellectual disability, obesity, and dysmorphic features. Cold Spring Harb. Mol. Case Stud. *2*, a001172.

White, S.M., Bhoj, E., Nellaker, C., Lachmeijer, A.M.A., Marshall, A.E., Boycott, K.M., Li, D., Smith, W., Hartley, T., McBride, A., et al. (2021). A DNA repair disorder caused by de novo monoallelic DDB1 variants is associated with a neurodevelopmental syndrome. Am. J. Hum. Genet. *108*, 749–756.

Winkler, D.D., and Luger, K. (2011). The histone chaperone FACT: structural insights and mechanisms for nucleosome reorganization. J. Biol. Chem. *286*, 18369–18374.

Wu, X., and Zhang, Y. (2017). TET-mediated active DNA demethylation: mechanism, function and beyond. Nat. Rev. Genet. *18*, 517–534.

Wysocka, J., Reilly, P.T., and Herr, W. (2001). Loss of HCF-1-chromatin association precedes temperature-induced growth arrest of tsBN67 cells. Mol. Cell. Biol. *21*, 3820–3829.

Yang, J., Zhang, X., Feng, J., Leng, H., Li, S., Xiao, J., Liu, S., Xu, Z., Xu, J., Li, D., et al. (2016). The histone chaperone FACT contributes to DNA replication-coupled nucleosome assembly. Cell Rep. *16*, 3414.

Zeman, M.K., and Cimprich, K.A. (2014). Causes and consequences of replication stress. Nat. Cell Biol. *16*, 2–9.

Zou, Y., Liu, Q., Chen, B., Zhang, X., Guo, C., Zhou, H., Li, J., Gao, G., Guo, Y., Yan, C., et al. (2007). Mutation in CUL4B, which encodes a member of cullin-RING ubiquitin ligase complex, causes X-linked mental retardation. Am. J. Hum. Genet. *80*, 561–566.

STAR★METHODS

KEY RESOURCES TABLE

REAGENT or RESOURCE	SOURCE	IDENTIFIER
Antibodies		
CUL4A	Abcam	ab72548, RRID:AB_1268363
HA (HRP conjugated)	Roche	11867423001, RRID:AB_390918
HA	Roche	12158167001, RRID:AB_390915
FLAG	Sigma	F1804, RRID:AB_262044
α-Tubulin	Sigma	T6074, RRID:AB_477582
CUL4B	Sigma	HPA011880, RRID:AB_1847340
SPT16	Santa Cruz Biotechnology	sc-28734, RRID:AB_661341
SPT16	BioLegend	607002, RRID:AB_315689
Myc (tag)	Santa Cruz Biotechnology	sc-40, RRID:AB_2857941
Cyclin A	Santa Cruz Biotechnology	sc-751, RRID:AB_631329
Cyclin B1	Santa Cruz Biotechnology	sc-245, RRID:AB_627338
DCAF14	Bethyl	A302-055A, RRID:AB_1604281
HSP90	BD	610418, RRID:AB_397798
β-Actin	CST	3700, RRID:AB_2242334
PARP	CST	9542, RRID:AB_2160739
His_6 (tag)	Recenttech	R4-TP1111
GST	Recenttech	R4-TM1222
To mouse IgG (HRP conjugated)	Promega	W4021, RRID:AB_430834
To rabbit IgG (HRP conjugated)	Promega	W4011, RRID:AB_430833
DDB1	Yue Xiong lab (University of North Carolina at Chapel Hill)	N/A
SSRP1	Santa Cruz Biotechnology	sc-25382, RRID:AB_2239916
γH2AX	Millipore	07-164, RRID:AB_310406
GAPDH	Fujifilm Wako	014-25524
Goat Anti-Rabbit IgG H&L (Alexa Fluor 488)	Abcam	ab150077, RRID:AB_2630356
Goat Anti-Rabbit IgG H&L (Alexa Fluor 594)	Abcam	ab150080, RRID:AB_2650602
Mouse IgG2a (isotype control)	MBL	M076-3, RRID:AB_593055
FLAG (HRP conjugated)	Abcam	ab49763, RRID:AB_869428
BrdU (FITC conjugated)	BD	347583, RRID:AB_400327
Chemicals, peptides, and recombinant proteins		
DAPI	Sigma	D9542
PEI MAX	Polysciences	24765-100
Thymidine	Fujifilm Wako	207-19421
Nocodazole	Fujifilm Wako	140-08531
Lipofectamine RNAiMAX	Invitrogen	13778030
Puromycin	Sigma	P8833
Hydroxyurea	Nacalai Tesque	18947-41
Dynabeads-protein G	ThermoFisher	DB10004
LR clonase II	Invitrogen	11791020
Glutathion-agarose	GE Healthcare	17-0756-04
Micrococcal nuclease	NEB	M0247S
Propidium iodide	BD	556463
Actinomycin D	Fujifilm Wako	018-21264

(*Continued on next page*)

Continued

REAGENT or RESOURCE	SOURCE	IDENTIFIER
Critical commercial assays		
EZClick Global RNA Synthesis Assay Kit	BioVision	K718
Deposited data		
RNA-seq (U2OS cells)	Coronel et al., 2021	GEO: GSE162163
RNA-seq (HeLa cells)	Ortmann et al., 2021	GEO: GSE169087
RNA-seq (HEK293T cells)	Bhattacharya et al., 2021	GEO: GSE151296
Experimental models: Cell lines		
U2OS	ATCC	CRL-3216
HEK293T	ATCC	CRL-3216
HeLa	ATCC	CCL-2
Oligonucleotides		
siCUL4A	Yue Xiong lab (University of North Carolina at Chapel Hill)	N/A
siCUL4B	Yue Xiong lab (University of North Carolina at Chapel Hill)	N/A
siDDB1	Yue Xiong lab (University of North Carolina at Chapel Hill)	N/A
Recombinant DNA		
pCMV-HA-Ubiquitin	Yue Xiong lab (University of North Carolina at Chapel Hill)	N/A
pcDNA3-3myc-CUL4A	Yue Xiong lab (University of North Carolina at Chapel Hill)	N/A
pcDNA3-3myc-CUL4B	Yue Xiong lab (University of North Carolina at Chapel Hill)	N/A
p3FLAG-puro-SUPT16H and its mutants	This study	N/A
pcDNA3-HA-Ubiquitin(WT)	This study	N/A
pcDNA3-HA-Ubiquitin(K6R)	This study	N/A
pcDNA3-HA-Ubiquitin(K11R)	This study	N/A
pcDNA3-HA-Ubiquitin(K27R)	This study	N/A
pcDNA3-HA-Ubiquitin(K29R)	This study	N/A
pcDNA3-HA-Ubiquitin(K33R)	This study	N/A
pcDNA3-HA-Ubiquitin(K48R)	This study	N/A
pcDNA3-HA-Ubiquitin(K63R)	This study	N/A
pENTR3C	Invitrogen	11817-012
pENTR3C-DCAF1	Yue Xiong lab (University of North Carolina at Chapel Hill)	N/A
pENTR3C-DCAF2	This study	N/A
pENTR3C-DCAF3	This study	N/A
pENTR3C-DCAF4	This study	N/A
pENTR3C-DCAF5	This study	N/A
pENTR3C-DCAF6	This study	N/A
pENTR3C-DCAF7	This study	N/A
pENTR3C-DCAF8	This study	N/A
pENTR3C-DCAF9	This study	N/A
pENTR3C-DCAF10	This study	N/A
pENTR3C-DCAF11	This study	N/A
pENTR3C-DCAF12	This study	N/A
pENTR3C-DCAF13	This study	N/A
pENTR3C-DCAF14	This study	N/A
pENTR3C-DCAF15	This study	N/A
pENTR3C-DCAF16	This study	N/A
pENTR3C-DCAF17	This study	N/A
pENTR3C-DDB2	This study	N/A
pENTR3C-CSA	This study	N/A
pENTR3C-GRWD1	This study	N/A
pENTR3C-H3.1	This study	N/A

(*Continued on next page*)

Continued

REAGENT or RESOURCE	SOURCE	IDENTIFIER
pENTR3C-H4	This study	N/A
pENTR3C-H3.1	This study	N/A
pENTR3C-H2A	This study	N/A
pENTR3C-SUPT16H	This study	N/A
pENTR3C-SSRP1	This study	N/A
pcDNA3-HA-DCAF1	Yue Xiong lab (University of North Carolina at Chapel Hill)	N/A
pCAG-puro-Myc-DCAF2	This study	N/A
pcDNA3-HA-DCAF3	This study	N/A
pcDNA3-HA-DCAF4	This study	N/A
pCAG-puro-Myc-DCAF5	This study	N/A
pCAG-puro-Myc-DCAF6	This study	N/A
pcDNA3-HA-DCAF7	This study	N/A
pcDNA3-HA-DCAF8	This study	N/A
pcDNA3-HA-DCAF9	This study	N/A
pCAG-puro-Myc-DCAF10	This study	N/A
pcDNA3-HA-DCAF11	This study	N/A
pcDNA3-HA-DCAF12	This study	N/A
pcDNA3-HA-DCAF13	This study	N/A
pCAG-puro-Myc-DCAF14	This study	N/A
pcDNA3-HA-DCAF15	This study	N/A
pCAG-puro-Myc-DCAF16	This study	N/A
pcDNA3-HA-DCAF17	This study	N/A
pcDNA3-HA-DDB2	This study	N/A
pCAG-puro-Myc-CSA	This study	N/A
pcDNA3-HA-GRWD1	This study	N/A
pET30-H3.1	This study	N/A
pET30-H4	This study	N/A
pGEX6P-SUPT16H	This study	N/A
pcDNA3-HA-H3.1	This study	N/A
pcDNA3-HA-H2A	This study	N/A
p3FLAG-puro-SSRP1	This study	N/A
pcDNA3-HA-SSRP1	This study	N/A
pBS-hSUPT16H(K674R)-KI TV	This study	N/A
pBS-LNL(loxP-Neo-LoxP)	This study	N/A
pMX-puro-Cre	Keiichi I. Nakayama lab (Kyushu University)	N/A
pcDNA3-HA-SSRP1	This study	N/A
pSpCas9-SUPT16H	This study	N/A
pSpCas9(BB)-2A-Puro (PX459)	Addgene	48139
pSpCas9-SUPT16H	This study	N/A
pSpCas9-DCAF14-1	This study	N/A
pSpCas9-DCAF14-2	This study	N/A
pSpCas9-DCAF14-3	This study	N/A
pSpCas9(BB)-2A-Puro (PX459)	Addgene	62988
Software and algorithms		
R-4.1.2	CRAN	https://cran.r-project.org
Image J 1.53e	NIH	https://imagej.nih.gov/ij
FlowJo	BD	https://www.flowjo.com
CRISPRDirect	Naito et al., 2015	https://crispr.dbcls.jp
RaNA-seq	Prieto and Barrios, 2019	https://ranaseq.eu

RESOURCE AVAILABILITY

Lead contact

Further information and requests for resources and reagents should be directed to and will be fulfilled by the lead contact, Keiko Nakayama (nakayak2@med.tohoku.ac.jp).

Materials availability

All reagents generated in this study are available from the lead contact.

Data and code availability

- This paper analyzes existing, publicly available data. These accession numbers for the datasets are listed in the key resources table. All data reported in this paper will be shared by the lead contact upon request.
- This paper does not report original code.
- Any additional information required to reanalyze the data reported in this paper is available from the lead contact upon request.

EXPERIMENTAL MODEL AND SUBJECT DETAILS

Cell culture

HeLa cells, U2OS cells, and HEK293T cells were maintained under 5% CO_2 at 37°C in Dulbecco's modified Eagle's medium (DMEM) supplemented with 10% fetal bovine serum, penicillin (50 U/mL), streptomycin (50 μg/mL), 2 mM L-glutamine, 1% MEM–nonessential amino acids, and 1% sodium pyruvate. All cell lines tested negative for mycoplasma contamination. Plasmid transfection was performed with the use of PEI MAX. Cells were synchronized in S phase by treatment twice with 2 mM thymidine (treatment for 19 h, release for 10 h, treatment for 15 h, and release for 4 h). Synchronization of cells in M phase was performed by treatment with nocodazole (100 ng/mL) for 14 h followed by mechanical shake-off.

METHOD DETAILS

Plasmid construction

Complementary DNAs encoding SPT16, SSRP1, DCAF1, DCAF2, DCAF3, DCAF4, DCAF5, DCAF6, DCAF7, DCAF8, DCAF9, DCAF10, DCAF11, DCAF12, DCAF13, DCAF14, DCAF15, DCAF16, DCAF17, DDB2, CSA, GRWD1, histone H2A, histone H3.1, and histone H4 were amplified from HEK293T cells, cloned into pENTR, and verified by sequencing. The resulting pENTR plasmids were recombined with destination plasmids as described previously (Nakagawa et al., 2015) with the use of LR clonase II. Deletion and point mutations were introduced by polymerase chain reaction (PCR)–mediated mutagenesis. The pSpCas9(BB)-2A-Puro vector was obtained from Addgene, and DNA fragments encoding guide RNAs for DCAF14 knockout were introduced individually as described previously (Ran et al., 2013). Target sequences in exon 1 of *DCAF14* were determined with the CRIPSRDirect website (Naito et al., 2015): 5′-AGGCCTCTCGGAGCTGCGAT-3′, 5′-TACCCGATCGCAGCTCCGAG-3′, and 5′-CCATAAACATGTCTTGTGAG-3′ [numbers 1–3, respectively (Figure 4B)]. Expression vectors for HA-ubiquitin, Myc-CUL4A, and Myc-CUL4B were described previously (Nakagawa and Xiong, 2011).

Immunoprecipitation

Cells were washed with phosphate-buffered saline (PBS) and lysed for 10 min at 4°C in NP-40 lysis buffer [0.5% Nonidet P-40, 50 mM Tris-HCl (pH 7.5), 150 mM NaCl, 10% glycerol, protease inhibitor cocktail (aprotinin at 10 μg/mL, leupeptin at 10 μg/mL, 1 mM phenylmethylsulfonyl fluoride), phosphatase inhibitor cocktail (0.4 mM sodium orthovanadate, 0.4 mM EDTA, 10 mM NaF, 10 mM sodium pyrophosphate)]. The lysates were centrifuged at 20,000 × g for 15 min at 4°C, and the resulting supernatants were incubated for 60 min at 4°C with Dynabeads–protein G conjugated with the required antibodies. The immune complexes were washed three times with PBS containing 0.1% Triton X-100 and 10% glycerol and were then subjected to SDS-polyacrylamide gel electrophoresis for immunoblot analysis.

Ubiquitylation assay

Ubiquitylation assays were performed as described previously (Nakagawa et al., 2018). Cells were transfected for 1 day with expression plasmids for FLAG-tagged SPT16 or SSRP1, HA-ubiquitin, and Myc epitope–tagged DCAF proteins as indicated, after which cell lysates were prepared with the NP-40 lysis buffer described above for immunoprecipitation but supplemented with 0.1% SDS in order to disrupt noncovalent protein-protein interactions. The lysates were then subjected to immunoprecipitation with antibodies to FLAG followed by immunoblot analysis with antibodies to HA.

RNA interference

Cells were transfected with CUL4A, CUL4B, or DDB1 siRNAs with the use of the Lipofectamine RNAiMAX reagent for 24 h before performance of the ubiquitylation assay. Target sequences were described previously (Nakagawa and Xiong, 2011).

In vitro binding assay

GST-tagged M domain and ubiquitin-fused M domain fragments of SPT16 as well as His_6-tagged H3.1 and H4 were isolated from *Escherichia coli* (BL21) transformed with corresponding pGEX6P or pET30 vectors as described previously (Nakagawa and Xiong, 2011). The *in vitro* pull-down assay was also performed as previously described (Yang et al., 2016), with minor modifications. The GST-SPT16-M or GST-Ub-SPT16-M fusion proteins (12 μg) were incubated with glutathione-agarose in buffer A150 [25 mM Tris-HCl (pH 7.5), 150 mM NaCl, 1 mM EDTA, 0.01% Triton X-100] for 2 h at 4°C, after which the beads were washed extensively with buffer A100 (same as A150 but containing 100 mM NaCl), divided into four portions, and incubated overnight at 4°C with the indicated amounts of the His_6-tagged H3.1 and H4 proteins in 500 μL of buffer A150. The beads were washed extensively with buffer A150, and the bound proteins were then eluted with SDS sample buffer and subjected to immunoblot analysis.

Immunofluorescence staining

Immunocytofluorescence staining was performed as described previously (Nakagawa et al., 2020), with some modifications. U2OS cells grown on glass coverslips were fixed for 10 min with 1% paraformaldehyde, washed with PBS, and permeabilized for 10 min with PBS containing 0.5% Triton X-100. They were then exposed to 5% nonfat milk in PBS before incubation with primary antibodies for 16 h at 4°C. After three washes with PBS containing 0.1% Tween-20 (PBS-T), the cells were incubated for 45 min at room temperature with AlexaFluor-conjugated secondary antibodies, washed with PBS-T, exposed to DAPI (5 μg/mL) for 1 min, and then examined with an BZ-9000 microscope (Keyence).

Generation of SPT16(K674R) knockin cells

A targeting vector [pBS-hSUPT16H(K674R)-KI TV] was constructed by PCR-mediated cloning of the 1-kbp region covering intron 15 to intron 17 (immediately upstream of nucleotide 21,360,706 on human chromosome 14 of the GRCh38/hg38 assembly) of *SUPT16H* (left arm) and the 1-kbp region containing intron 17 to intron 18 (immediately downstream of nucleotide 21,360,707 on chromosome 14 of GRCh38/hg38) of *SUPT16H* (right arm), followed by insertion of these fragments into the pBS-3FLAG-LNL (loxP-neo-loxP) vector. The PAM sequence and codon 674 were mutated as shown in Figure 5C. U2OS cells were transfected with the linearized targeting vector and pSpCas9-SUPT16H, which targets 5′-TAACCAACTGAGCTAACCGG-3′ as a protospacer and induces double-strand breaks in intron 17 of *SUPT16H*. After selection with G418 (400 μg/ml) for 6 days, the cells were transfected with pMX-puro-Cre, selected with puromycin (5 μg/mL) for 2 days, and then cloned by limiting dilution in 96-well plates. The resulting single cell–derived clones were screened for SPT16(K674R) knockin by genomic PCR analysis and sequencing. No homozygous knockin cells were obtained.

Chromatin fractionation

Chromatin fractionation was performed as described previously (Mendez and Stillman, 2000; Wysocka et al., 2001), with some modifications. HEK293T cells (2×10^6) that had been transfected with expression vectors for 2 days or U2OS cells (1×10^7) were suspended in buffer A [10 mM Tris-HCl (pH 8.0), 10 mM KCl, 1.5 mM $MgCl_2$, 0.34 M sucrose, 10% glycerol, 1 mM dithiothreitol, 0.1% Triton X-100] containing protease inhibitors, incubated for 8 min on ice, and subjected to centrifugation at 1300 × g for 5 min at 4°C. The nuclear pellet was washed once by recentrifugation in buffer A and then lysed in buffer B (3 mM EDTA, 0.2 mM EGTA, 1 mM dithiothreitol) containing protease inhibitors. Insoluble chromatin was isolated by centrifugation at 1700 × g for 5 min at 4°C, washed once by recentrifugation in buffer B, and incubated with micrococcal nuclease (4 U/mL) in buffer C [10 mM Tris-HCl (pH 8.0), 10 mM KCl, 1 mM $CaCl_2$] for 3 min at 37°C. The reaction was stopped with 1 mM EDTA, and the soluble chromatin fraction was obtained as the supernatant after centrifugation at 1700 × g for 5 min at 4°C. Whole cell extracts were prepared by ultrasonic treatment to disrupt DNA in radioimmunoprecipitation assay (RIPA) buffer [50 mM Tris-HCl (pH 8.0), 0.1% SDS, 150 mM NaCl, 1% NP-40, 0.5% sodium deoxycholate, protease inhibitor cocktail].

Colony formation assay

A colony formation assay was performed as described previously (Ishida et al., 2017). U2OS cells (5×10^2) were plated in 6-cm dishes, treated with the indicated concentrations of HU for 1 day, and then cultured for 2 weeks in the absence of HU. The cells were then fixed and stained with 4% Giemsa solution for assessment of colony formation. The number of colonies containing >50 cells was counted.

Cell counting

The population doubling level of cells was calculated by adding [log (cell number at passage) - log (cell number at previous passage)]/log (days during passage) at each passage as previously reported (Nakagawa et al., 2018).

Flow cytometry

Flow cytometry was performed as previously described (Funayama et al., 2017). U2OS cells were treated with 10 μM BrdU for 30 min at 37°C, fixed with ice-cold 70% ethanol for 30 min, and treated with a denaturing solution (2 M HCl containing 0.5% Triton X-100) for 30 min at 37°C. After exposure to 0.1 M sodium tetraborate decahydrate (pH 8.5) for 2 min at 37°C, the cells were stained with fluorescein isothiocyanate(FITC)–labeled antibodies to BrdU and propidium iodide for 30 min at 37°C and then analyzed with a FACSCanto II flow cytometer (BD Biosciences).

Analysis of transcriptomics data

Public transcriptomics data for U2OS (Coronel et al., 2021), HeLa (Ortmann et al., 2021), and HEK293T (Bhattacharya et al., 2021) cells were obtained from the NCBI Gene Expression Omnibus (GEO) database (GSE162163, GSE169087, and GSE151296, respectively). Transcripts per million (TPM) values for each cell line were calculated with the use of RaNA-Seq (Prieto and Barrios, 2019). TPM values of DCAF genes, SUPT16H, SSRP1, and AGRP were manually extracted, converted to $\log_2$[TPM], and represented as a heat map drawn with R. Standardized z-score was calculated with TPM values of DCAF genes, SUPT16H and SSRP1.

QUANTIFICATION AND STATISTICAL ANALYSIS

The number of biological replicates (n) as well as details of statistical analysis can be found in the figure legends. Quantitative data are presented as means ± SD. Statistical analysis was performed with the unpaired or paired two-tailed Student's *t* test (for comparison of two samples) or by one-way or two-way analysis of variance (ANOVA) followed by Tukey's test (for comparison of more than two samples). Excel and R software were used for *t* tests and for ANOVA and Tukey's test, respectively. A p value of <0.05 was considered statistically significant.